IL NUOVO CIMENTO **47 C** (2024) 180
DOI 10.1393/ncc/i2024-24180-2

Colloquia: HADRON2023

Measurement of the photoproduction cross-section for $\gamma p \to \phi\pi^+\pi^- p$ and search for the $Y(2175)$ at GlueX

K. Götzen(1) and F. Nerling(1)(2)(3)(*) on behalf of the GlueX Collaboration

(1) *GSI Helmholtzzentrum für Schwerionenforschung GmbH - Darmstadt, Germany*
(2) *Helmholtz Forschungsakademie Hessen für FAIR (HFHF), Campus Frankfurt - Frankfurt, Germany*
(3) *Goethe Universität Frankfurt am Main - Frankfurt, Germany*

received 21 December 2023

Summary. —
The $Y(2175)$, recently renamed to $\phi(2170)$, is one of the rare exotic candidates connected to strangeonium instead of the heavier charmonium-like and bottomonium-like exotic states. Originally observed in initial-state radiation by the BaBar experiment in 2006, it could be a strange partner of the famous charmonium-like exotic vector state $Y(4230)$. Various interpretations exist in the literature, such as conventional strangeonium, tetraquark or hybrid state. Meanwhile, it has been seen in different experiments and decay channels. The available experimental information obtained only from e^+e^- collider experiments is, however, not sufficient to confirm or disprove any of the proposed interpretations. Information about the production of this state in other processes is required. In this paper, we report on our measurement of the production cross-section of the reaction $\gamma + p \to \phi\pi^+\pi^- + p$ and the search performed for $Y(2175) \to \phi\pi^+\pi^-$ with the GlueX experiment.

1. – Introduction

Since the beginning of the millennium, numerous candidates of charmonium-like exotic XYZ states have been reported, such as the $X(3872)$, the $Y(4230)$ or the $Z_c(3900)$. The topic of exotic bound states of the strong interaction has thus gained new momentum, for a recent review see, *e.g.*, [1]. Recently renamed to $\chi_{c1}(3872)$ according to the new naming scheme by the PDG, the $X(3872)$, was the first of the XYZ states discovered in 2003 by the Belle experiment. The $Z_c(3900)^{\pm}$ is a manifestly exotic state, most presumably a four-quark state, and was first reported by BESIII. The supernumerary vector state $Y(4230)$ discovered by the BaBar experiment in initial state radiation (ISR) is, among other interpretations, suggested to be a molecular four-quark state or a charmonium hybrid state.

In the bottomonium sector, analogous exotic candidates have been reported as well. Though less conclusive, there has also been significant progress in the light-quark sector,

(*) Corresponding author. E-mail: F.Nerling@gsi.de

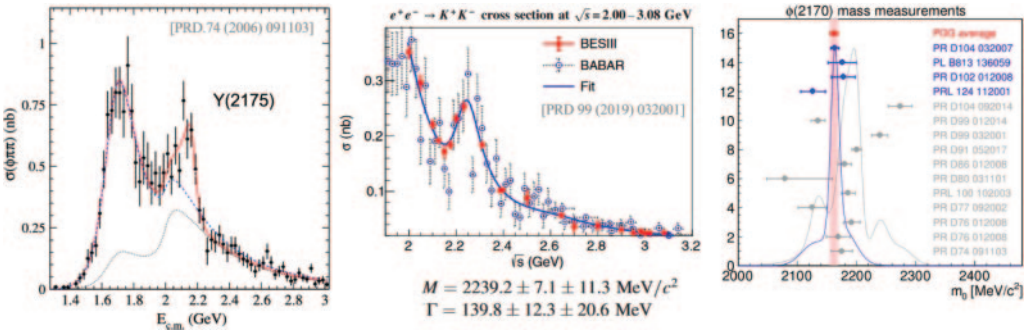

Fig. 1. – (Color online) Left: discovery plot of the $Y(2175)$ by BaBar. Centre: a measurement by BESIII. Right: compilation of individual measurements (not provided by PDG), summarised are all measurements listed by the PDG, and indicated by blue colour are those used by the PDG for their average values.

where promising light hybrid meson candidates, such as the $\pi_1(1600)$ and the $\pi_1(1400)$, had been studied for decades. Based on the largest data sets accumulated with the COMPASS experiment using a 190 GeV/c pion beam on a liquid hydrogen (proton) target, both P-wave structures observed in that data, the $\pi_1(1600) \to \eta'\pi$ and $\pi_1(1400) \to \eta\pi$, have been published from a partial-wave analysis of the 2008 COMPASS data [2]. This COMPASS result has recently been re-analysed in a coupled-channel analysis by JPAC, in which both the $\pi_1(1600)$ and the $\pi_1(1400)$ can be described by a single exotic π_1 resonant pole with $J^{PC} = 1^{-+}$ [3].

The $Y(2175)$, in the meantime renamed to $\phi(2170)$ by the PDG, was first reported by BaBar [4] (fig. 1 (left)), and has meanwhile been confirmed by different experiments and decay channels. This state is proposed to be the strange partner of the $Y(4230)$. The measured resonance parameters, such as the mass, vary significantly for the different measurements (fig. 1 (right)). A mass of about 2.24 GeV/c^2 (fig. 1 (centre)) has for instance been reported from a recent BESIII measurement [5], which is about 80 MeV/c^2 larger than the current PDG average value of 2162 MeV/c^2 [6]. Remarkably, all the available experimental information of the production of this state so far is restricted to e^+e^- experiments.

Given the many exotic candidates reported since 2003 in the heavy-quark sector as well as the latest results in the light-meson sector, and the progress on the theoretical side, new production mechanisms have to be explored to further pin down the nature of these states.

2. – The GlueX experiment at JLab

The GlueX experiment is dedicated to the study of such exotic states in photoproduction. It is operated at Jefferson Lab in the experimental Hall D (fig. 2 (left)). The electron beam provided by the Continuous Electron Beam Accelerator Facility (CEBAF) is converted into a linearly polarised photon beam using the coherent bremsstrahlung technique on a thin diamond radiator. The coherent peak is at about 9 GeV, where the degree of polarisation achieved is about 40%. The fixed-target spectrometer (fig. 2 (right)) is optimised to reconstruct a wide range of charged as well as neutral final-state particles.

Though mainly dedicated to map out and study exotic light hybrid mesons, GlueX offers unique capabilities and allows for access to states up to the charmonium region.

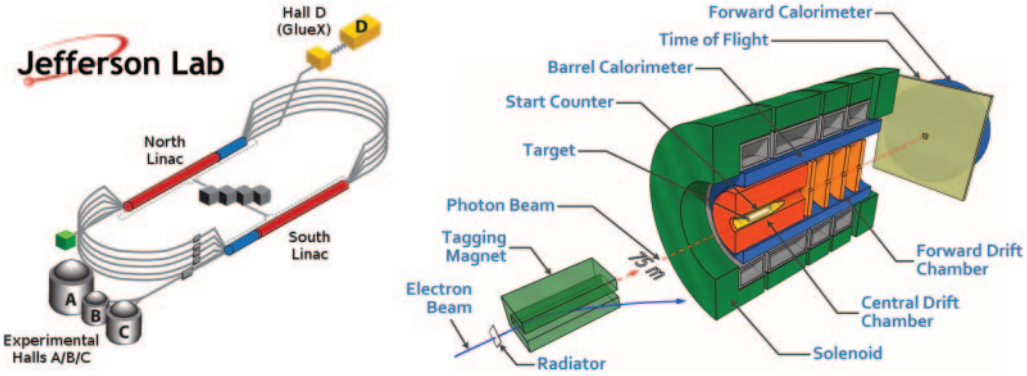

Fig. 2. – Left: overview of the CEBAF accelerator facility at Jefferson Lab; the GlueX experiment is located in Hall D. Right: the GlueX fixed-target experimental setup.

The GlueX Phase-I data analysed and presented here was collected in three different periods during 2017 and 2018. The corresponding integrated luminosity for $E_\gamma > 8\,\mathrm{GeV}$ is $304\,\mathrm{pb}^{-1}$ in total, namely $53\,\mathrm{pb}^{-1}$, $153\,\mathrm{pb}^{-1}$, and $98\,\mathrm{pb}^{-1}$ for the 2017, Spring 2018 and Fall 2018 data takings, respectively.

3. – Study of $\gamma p \to \phi\pi\pi p$ photoproduction

The $Y(2175)$ is predicted to be produced with a 8 GeV photon beam according to a theoretical calculation yielding a cross-section of about 1 nb [7]. Instead of the $\eta\phi$ decay channel addressed in that study, we have performed a measurement of the differential cross-section measurement for the $\phi\pi\pi$ decay channel to benefit from larger reconstruction efficiencies for charged final-state particles as well as an expected larger branching fraction.

3˙1. *Event selection of exclusive $\phi\pi\pi$ final states.* – The event selection consists in basically three parts. After applying merely loose particle identification (PID) based on $\mathrm{d}E/\mathrm{d}x$ and time-of-flight information, the $\gamma K^+K^-\pi^+\pi^- p$ event candidates are formed. A 4C kinematic fit of the $K^+K^-\pi^+\pi^- p$ to the γp system is applied together with a vertex fit. The following five event selection criteria are applied subsequently. We restrict ourselves to the photon beam energies $E_\gamma > 8\,\mathrm{GeV}$ (fig. 3 (left)), and the squared momentum transfer $-t < 1\,\mathrm{GeV}^2/c^4$ to reduce baryonic contributions (fig. 3 (centre)). To suppress Δ^{++}, a veto cut is applied by requiring $m(\pi^+ p) > 1.35\,\mathrm{GeV}/c^2$ (fig. 3 (right)). We ensure the exclusivity of the event sample by a missing mass cut of $|MM^2| < 50\,\mathrm{MeV}/c^2$ and a cut on the reduced chi-square of $\chi^2_{\mathrm{4C+vertex}} < 70/11$. The latter two cuts are optimised using the figure of merit of the ϕ signal in data. Finally, we determine the ϕ yield as a function of the $\phi\pi^+\pi^-$ mass and thus the yield of $\phi\pi^+\pi^-$ events as needed for the differential cross-section measurement. Since the cut on the momentum transfer $-t$ has been applied also on the MC generator level, the cross-section results presented are thus to be understood as "fiducial" measurements restricted to just this $-t$ range.

3˙2. *Differential photoproduction cross-section measurement.* – The reconstruction efficiencies as well as the ϕ yield are determined for 40 equidistant mass slices along the $\phi\pi^+\pi^-$ mass between $1.4\,\mathrm{GeV}/c^2$ and $3.2\,\mathrm{GeV}/c^2$. The efficiencies are obtained by dividing the number of reconstructed by the number of generated MC events for each

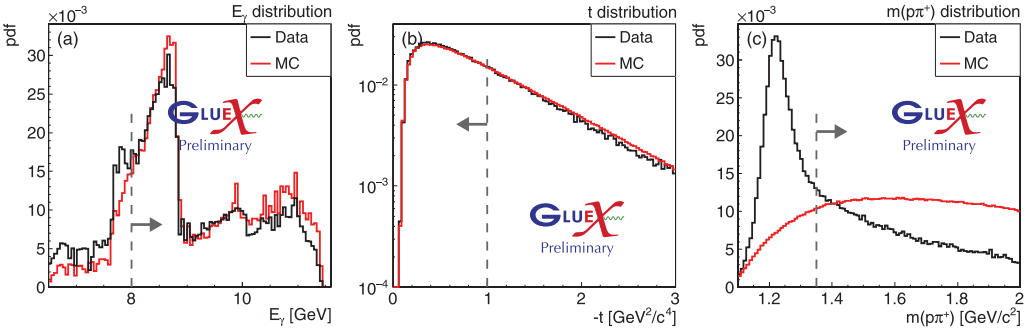

Fig. 3. – Reconstructed event distributions for MC-simulated and real data with the applied event selection cuts indicated. Left: beam photon energy E_γ distribution (a). Centre: distribution of the squared momentum transfer $-t$. Right: invariant mass of the $(p\pi^+)$ system.

mass bin, resulting in values of about 3% to 7% depending on the given data set (fig. 4 (left)). A clear ϕ signal band is visible in the $m(K^+K^-)$ *vs.* $m(K^+K^-\pi^+\pi^-)$ invariant mass together with the background present in the data, as shown for the 2018 Fall data (fig. 4 (centre)). We extract the $m(\phi\pi^+\pi^-)$ event yield by fitting the ϕ signal in these bins of $m(\phi\pi^+\pi^-)$. The ϕ signal in data is shown for the 2018 Fall data together with the signal fit function, which is a Voigtian plus an empirical phase space function to describe the background (fig. 4 (right)). The resonance parameters of the ϕ and the resolutions are thus obtained from the data and then fixed for the slice-wise fits to extract the ϕ yields.

Employing the the mass-dependent reconstruction efficiencies (fig. 4 (left)), we obtain from the slice-wise extracted ϕ yields (fig. 5 (left)) the differential mass-dependent $\phi\pi^+\pi^-$ cross-section for each of the three data sets (fig. 5 (centre)) according to the following formula with the measured photon flux F and the target thickness d_{target}:

$$\frac{\mathrm{d}\sigma}{\mathrm{d}m} = \frac{N_\phi(m_i)}{\epsilon(m_i)\cdot F\cdot d_{\text{target}}\cdot \mathcal{B}(\phi(1020)\to K^+K^-)}. \tag{1}$$

The cross-section measurements for each of the three data sets we combine by applying

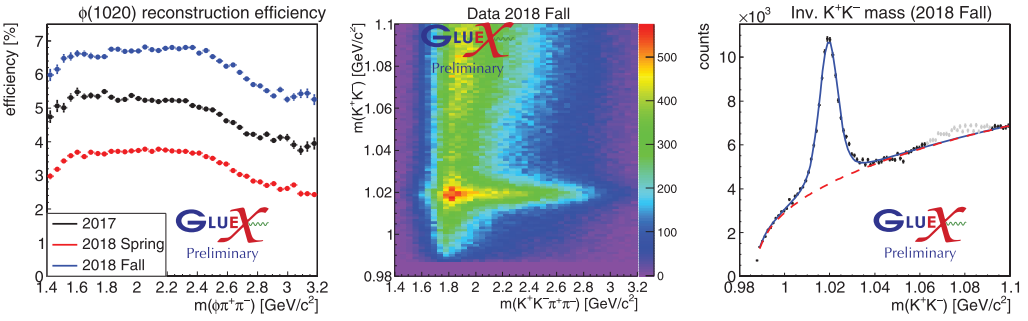

Fig. 4. – Left: reconstruction efficiencies as mass-dependently determined for the different data sets (a). Centre: invariant mass distribution $m(K^+K^-)$ *versus* $m(K^+K^-\pi^+\pi^-)$ exemplary shown for the "2018 Fall" data set (b). Right: accumulated ϕ peak in the "2018 Fall" data together with the ϕ and background model as applied with fixed parameters for the slice-wise fits to extract the ϕ yields from data.

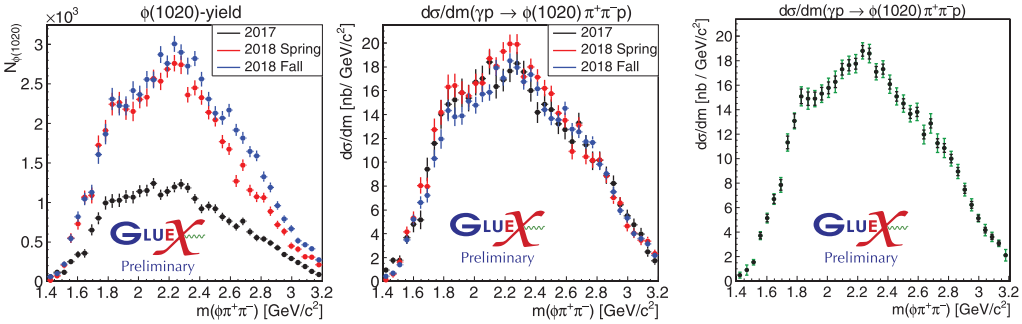

Fig. 5. – Left: extracted mass-dependent ϕ yields. Centre: differential cross-section for the different data sets (b). Right: final combined differential cross-section, including systematics; the outer error bars represent the total, and the inner ones the statistical uncertainties.

the weighted-average method [6], and obtain the resultant final mass-dependent differential cross-section measurement (fig. 5 (right)). The systematic errors are included in quadratic sum with the statistical ones (represented by the inner error bars), leading to the total (outer) errors bars. The sources as listed in table I have been considered to estimate the systematic uncertainties. The corresponding different cuts and values are accordingly varied, and for each variation the ϕ yield extraction and thus the complete cross-section measurement is repeated. To stay conservative, we take the difference in the resulting cross-section after each variation as compared to the default values and finally add all differences quadratically as the total systematic uncertainty.

3˙3. *Search for the $Y(2175)$ and further resonances in the measured cross-section.* – One of the main motivations for the cross-section measurement presented (fig. 5 (right)) is to address the $Y(2175)$ for the first time in photoproduction. As can be seen (fig. 5 (right)), we find a signal peak at around the $Y(2175)$ mass. We try to fit a signal shape for the $Y(2175)$ in $\mathrm{d}\sigma/\mathrm{d}m$ in form of a Voigtian function, using two different resonance parameters of mass and decay width together with a 4th-order Chebychev polynomial to describe the background. We take into account the mass resolution as obtained from the fits to the reconstructed MC-simulated data.

Additional systematic uncertainties are to be taken into account for this search,

TABLE I. – *Summary of systematic uncertainties considered for the cross-section measurement.*

Source	$\delta_{\mathrm{sys,avg}}$ [%]	Source	$\delta_{\mathrm{sys,avg}}$ [%]
$\phi(1020)$ branching ratio	1.0	χ^2 cut	0.9
MM^2 cut	0.4	Accidentals	0.5
K^+K^- binning	0.7	$\Delta(1232)^{++}$ veto	2.8
$\phi(1020)$ fit model data	0.8	$\phi(1020)$ fit model MC	0.7
$\phi(1020)$ fit range	1.6	$\phi(1020)$ veto range MC	0.5
$\phi(1020)$ integral range	0.1	$\phi(1020)$ param. interpolation	0.5
		Total systematic uncertainty	4.7

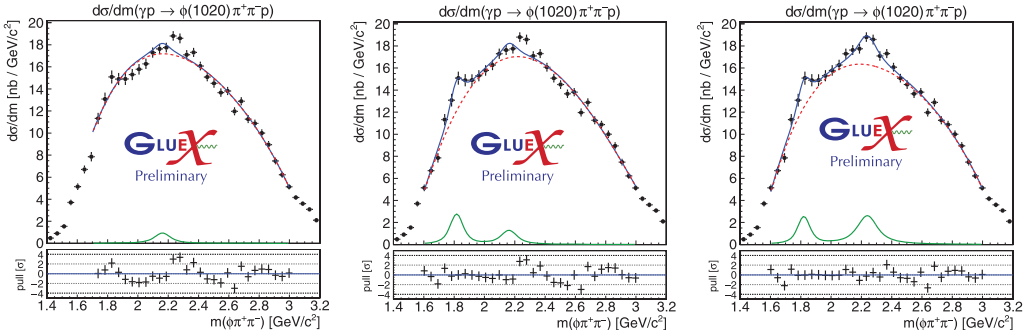

Fig. 6. – Search for the $Y(2175)$ and further resonances based on the measured differential photoproduction cross section. Left: fit model A_1 with one resonance $Y(2175)$ assuming the average resonance parameters quoted by the PDG . Centre: fit model A_2 with two resonances, the $Y(2175)$ assuming the average resonance parameters quoted by the PDG and a possible second structure at a mass of about 1.8 GeV/c^2. Right: fit model B_2 with two resonances, the $Y(2175)$ assuming the resonance parameters from the BESIII measurement [5] and a possible second structure at a mass of about 1.8 GeV/c^2.

namely the $m(\phi\pi\pi)$ fit range and the fit model itself, which are the resonance parameters and the background description. The parameters of width and mass we vary within $\pm 1\sigma$ of the quoted errors and also the degree of the Chebychev polynomial for the background description, and we subsequently repeat the fits. We take the (larger) difference as systematic uncertainty (to stay most conservative).

The fit model A_1 contains just one state described by a Breit-Wigner shape, the $Y(2175)$, using the fixed averaged values for mass and width quoted by the PDG [6]: $m_{\phi(2170)} = 2162 \pm 7\,\mathrm{MeV}/c^2$ and $\Gamma_{\phi(2170)} = 100^{+31}_{-21}\,\mathrm{MeV}$. The fit model B_1 contains a different state, namely a $Y(2239)$, using the values of mass and width as reported by the BESIII measurement mentioned above [5]: $m_{Y(2239)} = 2239.2 \pm 13.4\,\mathrm{MeV}/c^2$ and $\Gamma_{Y(2239)} = 139.8 \pm 24.0\,\mathrm{MeV}$. Moreover, we try also both fit models extended by an additional second state at lower mass (A_2, B_2).

In fig. 6, three out of these four different fit results are displayed. When employing fit model A_1 (fig. 6 (left)), one sees already by eye that the data is not well described, which is also reflected in the fit quality ($\chi^2/n = 2.78$). Adding a second possible structure at about $1.8\,\mathrm{GeV}/c^2$, *i.e.*, applying fit model A_2 (fig. 6 (left)) slightly improves the data description ($\chi^2/n = 2.74$), however, it does not improve the quality in describing the structure at about $2.2\,\mathrm{GeV}/c^2$. This peak is well described by the fit model B_1 for a $Y(2239)$ state ($\chi^2/n = 1.38$), *i.e.*, using the second set of resonance parameters [5]. Finally, when employing fit model B_2, *i.e.*, allowing for a second possible structure at about $1.8\,\mathrm{GeV}/c^2$ in addition to the $Y(2239)$, the description of the data is further improved ($\chi^2/n = 1.2$).

The resultant significances of the $Y(2239)$ vary from $Z_{\mathrm{tot}} = 5.7\,\sigma$ ($Z_{\mathrm{stats}} = 6.0\,\sigma$) to $Z_{\mathrm{tot}} = 4.7\,\sigma$ ($Z_{\mathrm{stats}} = 5.1\,\sigma$), depending on the applied fit model B_1 and B_2, respectively. While we do not find a significant signal for a $Y(2175)$ with resonance parameters quoted by the PDG, we observe for the first time a denoted $Y(2239)$ decaying to $\phi\pi^+\pi^-$ in photoproduction with a statistical significance of about 5σ with systematic uncertainties taken into account. The results of the search we performed are summarised in table II.

We find the measured production strength of the $Y(2239)$ to be reasonably consistent with the theoretical prediction of 1 nb, keeping in mind the fiducial measurement does

TABLE II. – *Summary of our search for the $Y(2175)$ in photoproduction: measured production cross-sections σ [pb], upper limits at the 90% confidence level UL [pb] and significances without (Z_{stats}) and with (Z_{tot}) systematic uncertainties.*

Fit model	Cross-section σ [pb]	UL [pb]	Z_{stats}	Z_{tot}
One-resonance fit (A_1), $Y(2175)$ fixed	$174 \pm 69 \pm 218$	499	2.1	1.6
Two-resonance fit (A_2), $Y(2175)$ fixed	$232 \pm 68 \pm 91$	379	1.8	1.5
One-resonance fit (B_1), $Y(2239)$ fixed	$641 \pm 82 \pm 181$	896	6.0	5.7
Two-resonance fit (B_2), $Y(2239)$ fixed	$232 \pm 68 \pm 91$	826	5.1	4.7

not represent the total production cross-section. Furthermore, we find strong evidence for a second structure at a mass of about $1.8\,\text{GeV}/c^2$. Though we do not quote fitted resonance parameters of this possible second state, we compute upper limits for such a state, resulting in $\sigma_{\text{UL(CL90)}} < 615\,\text{pb}$ (A_2) and $\sigma_{\text{UL(CL90)}} < 701\,\text{pb}$ (B_2), respectively, depending on the fit model.

4. – Summary

A first measurement of the differential photoproduction cross-section $\mathrm{d}\sigma/\mathrm{d}m$ for $\gamma p \to \phi\pi^+\pi^- p$ has been provided by the GlueX experiment. The $Y(2175)$, which is a candidate for the strange-quark partner of the $Y(4230)$, has been addressed for the first time in photoproduction based on this cross-section measurement.

When using the PDG average values as (fixed) resonance parameters, we do not find evidence ($Z_{\text{tot}} < 3$) for the $Y(2175)$. Using alternative parameters as measured by BESIII, we observe a significant signal between $Z_{\text{tot}} = 5.7\sigma$ and $Z_{\text{tot}} = 4.7\sigma$, depending on the fit model applied. The measured signal strength of the $Y(2239)$ is found to be consistent with theoretical predictions for photoproduction of the $Y(2175)$. Moreover, we find evidence for a second structure at a mass of about $1.8\,\text{GeV}/c^2$. For such a second state we provide upper limits that compute to $\sigma_{\text{UL(CL90)}} < 615\,\text{pb}$ and $\sigma_{\text{UL(CL90)}} < 701\,\text{pb}$, depending on the fit model applied.

REFERENCES

[1] BRAMBILLA N. *et al.*, *Phys. Rep.*, **873** (2020) 1.
[2] COMPASS COLLABORATION (ADOLPH C. *et al.*), *Phys. Lett. B*, **740** (2015) 303.
[3] JPAC COLLABORATION (RODAS A. *et al.*), *Phys. Rev. Lett.*, **122** (2019) 042992.
[4] BABAR COLLABORATION (AUBERT B. *et al.*), *Phys. Rev. D*, **74** (2006) 091103.
[5] BABAR COLLABORATION (ABLIKIM M. *et al.*), *Phys. Rev. D*, **99** (2019) 032001.
[6] PARTICLE DATA GROUP (WORKMAN R. L. *et al.*), *Prog. Theor. Exp. Phys.*, **8** (2022) 083C01.
[7] ZHAO C.-G. *et al.*, *Phys. Rev. D*, **99** (2019) 114014.